Functional Characterization of a Small Conductance GIRK Channel in Rat Atrial Cells

Emil N. Nikolov and Tatyana T. Ivanova-Nikolova
Department of Pharmacology and Toxicology, Brody School of Medicine, East Carolina University, Greenville, North Carolina

ABSTRACT Muscarinic K^+ (K_{ACh}) channels are key determinants of the inhibitory synaptic transmission in the heart. These channels are heterotetramers consisting of two homologous subunits, G-protein-gated inwardly rectifying K^+ (GIRK)1 and GIRK4, and have unitary conductance of ~35 pS with symmetrical 150 mM KCl solutions. Activation of atrial K_{ACh} channels, however, is often accompanied by the appearance of openings with a lower conductance, suggesting a functional heterogeneity of G-protein-sensitive ion channels in the heart. Here we report the characterization of a small conductance GIRK (scGIRK) channel present in rat atria. This channel is directly activated by $G\beta\gamma$ subunits and has a unitary conductance of 16 pS. The scGIRK and K_{ACh} channels display similar affinities for $G\beta\gamma$ binding and are frequently found in the same membrane patches. Furthermore, $G\beta\gamma$-activated scGIRK channels—like their K_{ACh} counterparts—exhibit complex gating behavior, fluctuating among four functional modes conferred by the apparent binding of a different number of $G\beta\gamma$ subunits to the channel. The electrogenic efficacy of the scGIRK channels, however, is negligible compared to that of K_{ACh} channels. Thus, $G\beta\gamma$ subunits employ the same signaling strategy to regulate two ion channels that are apparently endowed with very different functions in the atrial membrane.

INTRODUCTION

Autonomic regulation of the heart rate is a continuous process integrating multiple cellular events controlled by sympathetic and parasympathetic signals to the heart. Both branches of the autonomic nervous system rely on G-protein-coupled receptors and their downstream effectors to accomplish the control of cardiovascular function. Among these effectors, the K_{ACh} channels of the sinoatrial node and atria play a prominent role in the inhibitory synaptic transmission in the heart and slowing of the heart rate (Wickman et al., 1998; Yamada, 2002).

The cardiac K_{ACh} channels consist of two homologous subunits, G-protein-gated inwardly rectifying K^+ (GIRK)1 (Dascal et al., 1993; Kubo et al., 1993) and GIRK4 (Krapivinsky et al., 1995a). The GIRK1 and GIRK4 subunits form heterotetrameric channels with a $(GIRK1)_2(GIRK4)_2$ stoichiometry (Silverman et al., 1996, Tucker et al., 1996) and pore conductance of ~35 pS with symmetrical 150-mM KCl solutions. Topologically consistent with the bacterial KcsA K^+ channel (Doyle et al., 1998), each GIRK subunit comprises two transmembrane helixes (TM1, TM2) interrupted by a P region, and cytoplasmic NH_2- and COOH-terminal domains. The transmembrane helixes and the P regions form an integral transmembrane pore (Doyle et al., 1998), which is significantly extended by a tetrameric cytoplasmic pore formed by the NH_2- and COOH-terminal domains of the GIRK subunits (Nishida and MacKinnon, 2002). The activation of the K_{ACh} channels is conferred by direct $G\beta\gamma$ binding, apparently to multiple domains, on the intracellular surface of the channel (for reviews see Yamada et al., 1998, and Sadja et al., 2003). $G\beta\gamma$-activated K_{ACh} channels exhibit complex gating behavior, fluctuating among four functional modes conferred by the apparent binding of a different number of $G\beta\gamma$ subunits to four identical and independent sensors in the protein complex (Ivanova-Nikolova et al., 1998). This $G\beta\gamma$-dependent K_{ACh} channel gating is further complicated by slow modal transitions (on a timescale of minutes), which are independent of $G\beta\gamma$ concentration and probably involve some membrane-delimited processes (Yakubovich et al., 2000). At this time, the structural principles governing such complex K_{ACh} channel gating are not fully understood. Mutational studies of the transmembrane helixes of GIRK suggest that upon gating the TM2 helixes undergo both rotation (Yi et al., 2001) and bending at a conserved glycine residue (Jin et al., 2002, Jiang et al., 2002). Surprisingly, the structure of the cytoplasmic GIRK pore connects more realistically to an open conformation of the transmembrane pore than to a closed one (Nishida and MacKinnon, 2002). This structure identifies an additional possibility for channel activation—gating at the cytoplasmic pore—in the presence of a permanently open transmembrane pore of the GIRK channels.

Whereas the $G\beta\gamma$ subunits govern the gating phenomenon, the $G\alpha_i$ subunits have significant ramifications for the fidelity of coupling between different G-protein-coupled receptors and GIRK channels (Leaney et al., 2000). In addition, the $G\alpha_i$ subunits are responsible for termination of the G-protein signaling to the K_{ACh} channel (Doupnik et al., 1997; Saitoh et al., 1997; Peleg et al., 2002).

Submitted January 5, 2004, and accepted for publication August 12, 2004.

Address reprint requests to Tatyana T. Ivanova-Nikolova, Dept. of Pharmacology and Toxicology, Brody School of Medicine, East Carolina University, Greenville, NC 27858. Tel.: 252-744-2757; Fax: 252-744-3203 E-mail: ivanovanikolovat@mail.ecu.edu.

0006-3495/04/11/3122/15 $2.00

doi: 10.1529/biophysj.104.039487

In the atria, the heterotetrameric GIRK1/GIRK4 channels coexist with GIRK4 homomultimers of yet unidentified biological function (Corey and Clapham, 1998). The biochemical heterogeneity of atrial GIRK multimers is accompanied by a functional variability of G-protein-sensitive ion channels. Our examination of receptor-activated K_{ACh} channels in neonatal rat atrial myocytes frequently revealed the presence of two types of channel openings, one with a conductance of 34 pS and another one with a conductance of ~16 pS (with symmetrical 150-mM KCl solutions). Although these two conductance levels could be distinguished in K_{Ach} channel recordings from different species in a number of studies from other laboratories (Ito et al., 1991; Sui et al., 1996), the relation between the 34-pS and 16-pS events has never been investigated. These observations prompted us to investigate the 16-pS channel openings and their dependence on Gβγ. Here we define the properties of a previously uncharacterized Gβγ-sensitive inwardly rectifying K^+ channel observed in the membrane of rat atrial myocytes. This channel exhibits a small conductance (13–17 pS), fast kinetics, and, like the K_{ACh} channel, is directly activated by the Gβγ subunits. On the basis of the small conductance and mode of activation, we designated this channel scGIRK channel. Mechanistically, the activation of the scGIRK channels by Gβγ replicates the activation of the K_{ACh} channels, strengthening the notion that Gβγ-driven control of multiple functional states, evolving from the same effector molecule, is a common mechanism of signal transduction. The electrogenic efficacy of the scGIRK channel, however, is negligible compared to that of the K_{ACh} channel. Thus, these two channels are most probably endowed with very different physiological functions in the membrane of the atrial myocytes.

MATERIALS AND METHODS

Isolation and cell culture of neonatal cardiac myocytes

Experiments were performed on Sprague-Dawley rat atrial cells. Neonatal animals were cryoanaesthetized on ice and then decapitated. The heart was rapidly excised and the atrial tissue was removed for further dissociation. Primary cultures of rat atrial myocytes were obtained according to previously established procedures (Foster et al., 1990). Briefly, the atrial tissue was minced and treated with a mixture of trypsin, chymotrypsin, and elastase at 37°C. The suspension of dissociated cells was centrifuged through Percoll step gradients to obtain cell preparations consisting of >94% myocytes. The myocytes were suspended in modified Eagle's medium containing 5% newborn calf serum and 0.1 mM 5-bromo-2′-deoxyuridine and were plated on round (7 mm in diameter) gelatin-coated coverslips in culture dishes at a density of 1×10^5 cells/cm^2. After an overnight incubation, the cells were washed to remove nonadherent cells and cultured in a defined serum-free media 4 additional days.

Expression and purification of G-protein $\beta_1\gamma_7$ dimers followed the method developed by Kozasa and Gilman (1995) for purification of $\beta_1\gamma_2$ and has been previously described (Ivanova-Nikolova et al., 1998).

Electrophysiology

Single-channel currents through K_{ACh} and scGIRK channels were recorded from cell-attached and inside-out patches of atrial myocytes using the standard high-resolution patch-clamp method (Hamill et al., 1981). The membrane potential was zeroed with the following bath solution (in mM): 150 KCl, 5 EGTA, 5 glucose, 1.6 $MgCl_2$, 5 HEPES (pH 7.4). Pipette solution contained (in mM): 150 KCl, 1 $CaCl_2$, 1.6 $MgCl_2$, 5 HEPES (pH 7.4). Patch pipettes were made from borosilicate glass (World Precision Instruments, Sarasota, FL) on a Flaming Brown micropipette puller (Sutter Instrument, Novato, CA) and firepolished on a microforge (Narishige Scientific Instrument Lab, Tokyo, Japan). The resistance of the patch pipettes (when filled with pipette solution) was 10–20 MΩ. To estimate the number of K_{ACh} channels present in each patch, the atrial m_2-muscarinic receptors were activated with 1 μM acetylcholine added to the pipette solution, and the K_{ACh} channel activity was monitored in cell-attached configuration for 3–6 min. Patches with superimposed 34 pS-openings were not subjected to further investigation. Single-channel currents were recorded with a Patch Clamp List-Medical EPC-7 amplifier (ALA Scientific Instruments, Westbury, NY) using a DigiData 1200 series interface and pCLAMP 6.0 software, both from Axon Instruments (Foster City, CA). Data were digitized at 5 kHz and stored on a computer for further analysis. Some of the data were additionally filtered with an 8-pole Bessel filter (Frequency Devices, Haverhill, MA) at 2 kHz. The fast and slow time constants, $\tau_{o1} = 0.29 \pm 0.07$ ms and $\tau_{o2} = 1.1 \pm 0.3$ ms ($n = 9$ cells), derived from the open-time distributions of the filtered data were not significantly different from the time constants, $\tau_{o1} = 0.31 \pm 0.05$ ms and $\tau_{o2} = 1.3 \pm 0.2$ ms ($n = 8$ cells), estimated from unfiltered recordings of the elementary currents at the same membrane potential.

Only recordings with current transitions to a single 16-pS and/or a single 35-pS level (monitored for at least 10 min in the presence of Gβγ) were included in the analyses of the amplitude of channel openings, open dwell times, and gating modes. All-points amplitude histograms were generated using pCLAMP 6.0 software and fitted with the sum of several Gaussian functions to determine the mean current amplitude for the scGIRK and K_{ACh} channels. Lists of durations of single-channel events were generated by the FETCHAN Events List function using the half-amplitude threshold-crossing algorithm. Cumulative histograms of open dwell times were generated and fitted with the sum of two exponential components.

Examination of long episodes of single-channel data recordings at a constant $G\beta_1\gamma_7$ concentration frequently revealed the presence of slow modal transitions in scGIRK and of K_{ACh} channel gating, analogous to the slow gating transitions described for heterologously expressed GIRK1/4 channels (Yakubovich et al., 2000) but on a much slower timescale. Such transitions between different phases of channel activity were always associated with a change in the frequency of channel gating. Therefore, each recording was divided into 400-ms consecutive segments, and the frequency of apparent openings, f, was calculated for each segment. The 400-ms duration of the individual data segments was selected to reflect the mean burst duration of K_{ACh} channels exhibiting well-delineated bursting behavior; the same time interval was used for our analysis of the scGIRK channels. The mean frequency, F, was averaged over 30-s data recordings (from 75 consecutive 400-ms data segments) and plotted versus time (see Fig. 10, *A* and *B*). The resulting F-t plots accurately identified the apparently homogeneous sections of each recording. A data recording (usually longer than 6–7 min) was judged as homogeneous if the mean F values (denoted by the horizontal lines in Fig. 10, *A* and *B*) calculated from the first and the second halves of this recording were statistically indistinguishable.

RESULTS

Evidence for the presence of scGIRK channels in neonatal rat atrial myocytes

Inspection of individual atrial K_{ACh} channels activated in cell-attached patches by 1 μM ACh revealed the presence of

two populations of single-channel openings as illustrated in Fig. 1. One population exhibited a unitary conductance of 34 ± 1 pS ($n = 14$), characteristic of classical K_{ACh} channels, whereas the other population had a unitary conductance of 16 ± 1 pS ($n = 14$).

Patch excision in GTP-free solution completely abolished the activity of both the 16-pS and 34-pS events (Figs. 1 and 2), indicating the absence of an obligatory component required for channel gating in the cell-free membrane. Subsequent perfusion of the cytoplasmic side of the membrane with nanomolar concentrations of purified recombinant $G\beta_1\gamma_7$ restored the activity of both channels. Thus, a sole elevation in free membrane concentration of $G\beta\gamma$ was sufficient to activate not only the K_{ACh} channels, but the 16-pS events as well.

Examination of the gating pattern of the 16-pS events (Fig. 2) revealed a strong resemblance to the behavior of the canonical K_{ACh} channels. The 16-pS events, like their 34-pS counterparts, fluctuated between singular openings preceded and followed by long closed intervals and clusters of relatively closely spaced openings. Direct transitions between the 16-pS and the 34-pS conductance levels, however, were not detected even during long episodes (20–30 min) of single-channel data recordings. In addition, membrane patches harboring exclusively the 16-pS $G\beta\gamma$-activated events were frequently found (Fig. 2). These observations suggest that the 16-pS openings might result from activation of a previously uncharacterized atrial channel rather than from transitions to a subconductance state of the K_{ACh} channel. Furthermore, to the best of our knowledge there are no published data describing subconductance states of K_{ACh} channels.

To determine the voltage dependence of the small conductance events, current amplitudes were measured in symmetrical 150-mM KCl solutions at different membrane potentials and compared to those of K_{ACh} channels found in the same membrane patches (Fig. 3 *A*). The current-voltage plot (Fig. 3 *B*) generated from such experiments demonstrates that the 16-pS events, like the K_{ACh} channels, display inward rectification. Although the molecular identity of the 16-pS events is unknown, on the basis of their small conductance, direct $G\beta\gamma$ activation, and inward rectification, we designated these events ''small conductance (sc) GIRK channels'' for clarity of presentation.

To identify the elementary open states entered by the scGIRK channels, we generated distributions of open-interval durations at different (1.6–12 nM) $G\beta_1\gamma_7$ concentrations. The adequate fit of the open-time distributions (Fig. 4 *A*) invariably required a sum of two exponential components characterized by mean time constants, τ_{o1} and τ_{o2}, of 0.31 ms and 1.3 ms, respectively. Both τ_{o1} and τ_{o2} were independent of the $G\beta\gamma$ concentration. Similar analysis of K_{ACh} channels, activated in the same range of $G\beta_1\gamma_7$ concentration, yielded fast and slow open-time constants that were threefold greater ($\tau_{o1} = 0.93 \pm 0.14$ ms and $\tau_{o2} = 4.3 \pm 0.6$ ms, $n = 10$) than those estimated for the scGIRK channel.

The fast open-time constants estimated for the $G\beta\gamma$-activated scGIRK channels give rise to an important concern that the 16-pS events might represent distorted brief 34-pS openings rather than genuine events. To rule out this possibility we investigated the effect of cyclic adenosine monophosphate-dependent protein kinase (PKA) on scGIRK

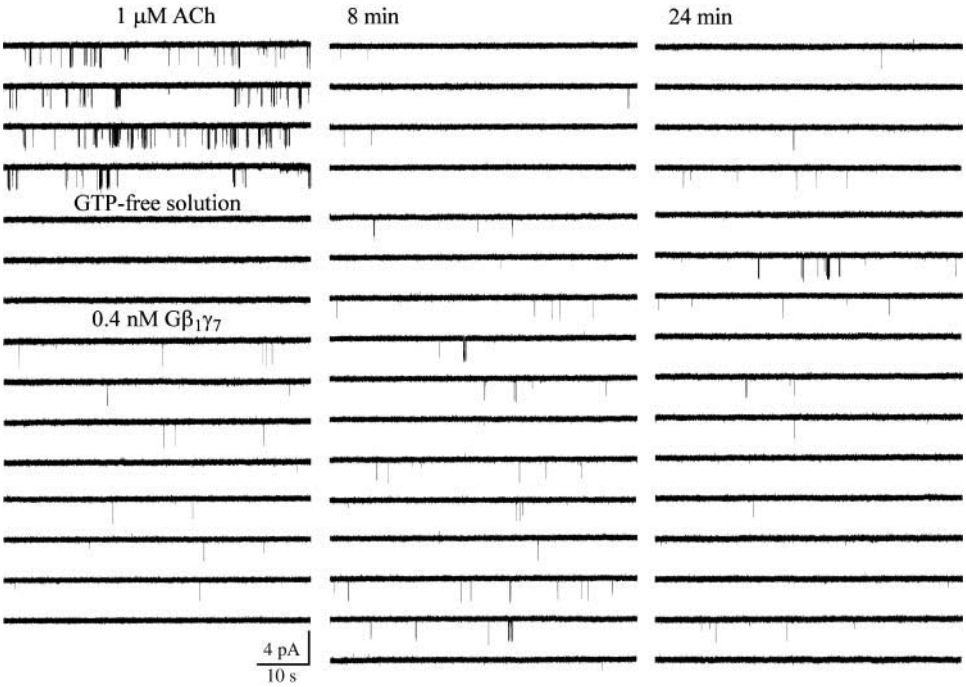

FIGURE 1 Two populations of G-protein-activated single-channel openings in neonatal rat atrial myocytes. Activation of a single 34-pS K_{ACh} channel in a cell-attached patch is accompanied by the appearance of 16-pS openings. In this and all following figures, the downward deflections correspond to inward currents. Membrane potential: −90 mV; 1 μM ACh is added to the pipette solution. Excision of the membrane patch in GTP-free solution instantaneously and completely eliminated both 16- and 34-pS events. The membrane potential continued to be clamped at −90 mV during the entire experiment. Perfusion of the experimental chamber with 0.4 nM $G\beta_1\gamma_7$ restored both the 16- and 34-pS single-channel openings. The single-channel recording in the presence of $G\beta_1\gamma_7$ begins 10 min after $G\beta_1\gamma_7$ application.

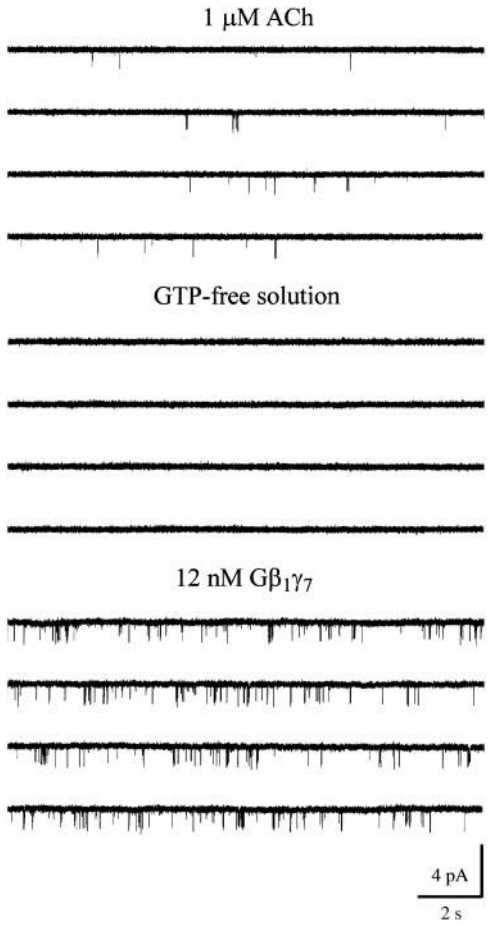

FIGURE 2 Small conductance atrial GIRK channel. Single-channel activity recorded in cell-attached configuration from an atrial myocyte in the presence of 1 μM ACh. Channel activity ceased after patch excision in GTP-free solution. Application of 12 nM $G\beta_1\gamma_7$ restored the channel activity. Membrane potential: −90 mV.

channel activation by $G\beta\gamma$. Since PKA phosphorylation significantly increases K_{ACh} channel open times (Kim, 1990; Mullner et al., 2003), it is expected to eliminate the 16-pS events from our recordings if they were poorly resolved, brief 34-pS events. Pairs of scGIRK and K_{ACh} channels residing in the same membrane patch were activated by purified recombinant $G\beta\gamma$, and then purified PKA catalytic subunit was applied to the cytoplasmic side of the patch in the presence of Mg-ATP. PKA_c application (200 pg/μl) caused a substantial upregulation of $G\beta\gamma$-activated scGIRK channels, which is illustrated in Fig. 4 ($n = 4$). The effect of PKA_c on scGIRK channel activity was observed within 3–6 min after PKA application and was sustained for the duration of our experiments. In control experiments, perfusion of $G\beta_1\gamma_7$-activated scGIRK and K_{ACh} channels with either Mg-ATP or heat inactivated PKA_c had no effect on the channel activity (data not shown). Comparison of the open-time distributions revealed that PKA potentiation of the scGIRK channel activity was associated with a twofold increase in both the fast and slow open-time constants ($\tau_{o1} = 0.66 \pm 0.08$ ms and $\tau_{o2} = 3.08 \pm 0.52$ ms, $n = 4$). Furthermore, PKA induced significant shift in the scGIRK channel gating toward a high open probability mode that was infrequently accessible in the presence of $G\beta_1\gamma_7$ alone (see Gating mechanism of scGIRK channels). At the same time, the unitary conductance of scGIRK channels was not affected in the presence of PKA_c (Fig. 4), thus eliminating the possibility that the 16-pS events result from very brief distorted K_{ACh} channel openings.

In summary, our analysis of unitary currents recorded from membrane patches either after m_2-receptor stimulation, or application of purified $G\beta_1\gamma_7$ subunits revealed the presence of ~16-pS channel openings with open durations threefold briefer than those of the canonical K_{ACh} channels activated under the same conditions. Our data also indicate that the activity of the scGIRK channels and their sensitivity to G-protein stimulation is efficiently regulated by PKA.

Gating mechanism of scGIRK channels

To understand the gating mechanism of scGIRK channels, we analyzed channel behavior at $G\beta_1\gamma_7$ concentrations ranging from 0.4 to 12 nM. Consistent with our previous observations using $G\beta_1\gamma_5$, the activation of both scGIRK and K_{ACh} channels by $G\beta_1\gamma_7$ developed gradually over the course of 6–10 min before reaching a sustained level of activity. To provide sufficient time for $G\beta_1\gamma_7$ incorporation in the membrane and to ensure a consistency of experimental

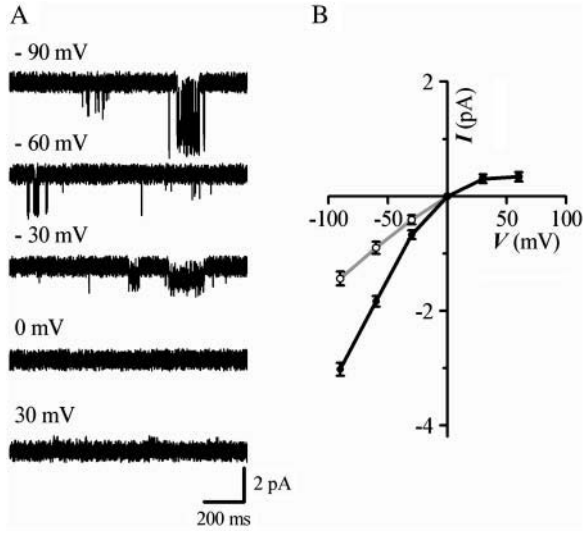

FIGURE 3 Voltage dependence of scGIRK and K_{ACh} channels. (*A*) $G\beta_1\gamma_7$-activated single-channel currents were recorded from the same membrane patch at the indicated potentials. All-points histograms were generated from the recordings and fitted by a sum of Gaussian functions to determine the mean current amplitudes. (*B*) I−V curves for the scGIRK (*gray*) and K_{ACh} (*black*) channels were constructed from the single-channel current amplitudes determined at each membrane potential. Each data point represents the mean ± SEM of currents recorded from 5 to 14 channels.

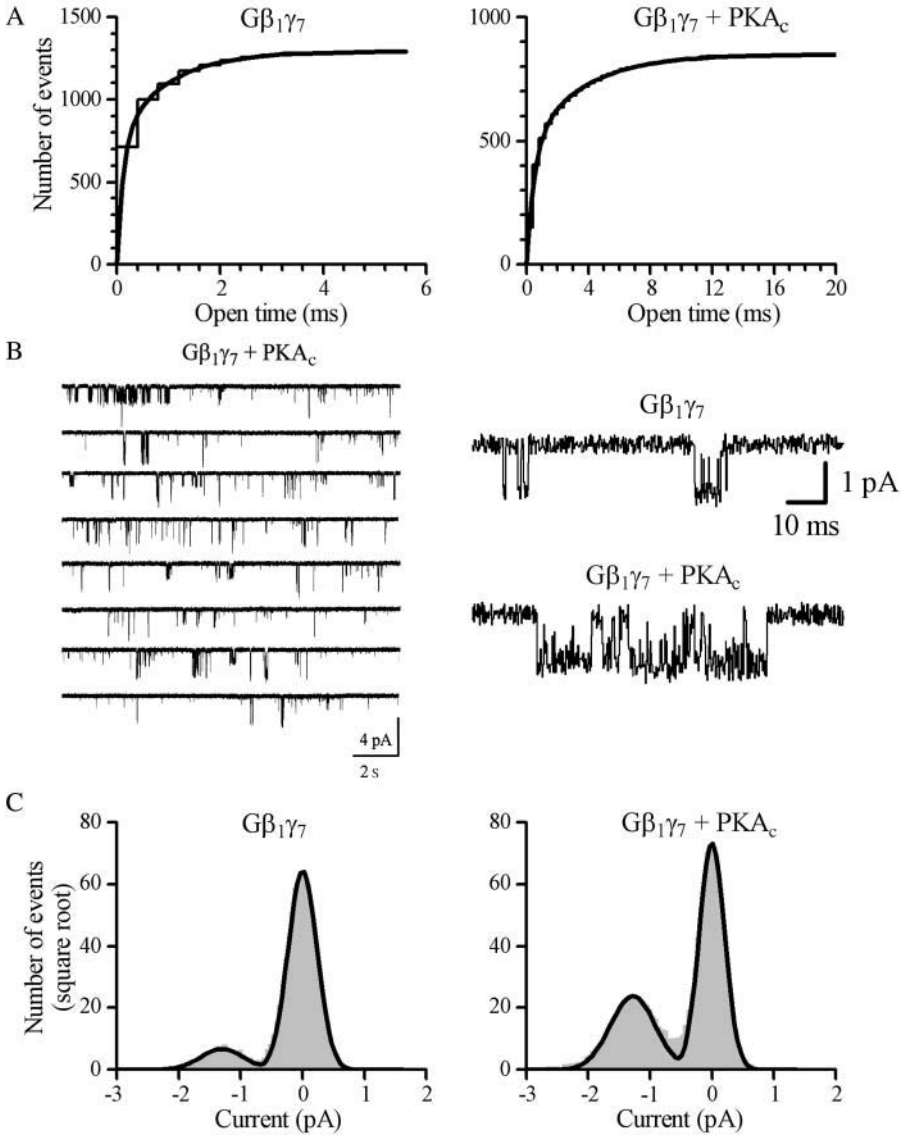

FIGURE 4 Characteristics of scGIRK channels. (*A*) Cumulative open-time distributions with superimposed fits are shown for two different scGIRK channels activated by 4 nM $G\beta_1\gamma_7$ in the absence (*left panel*) and presence (*right panel*) of Mg-ATP/PKA_c (the scGIRK channel shown in *B*). Membrane potential: −90 mV. Two exponential components were readily identified in both histograms. The time constants of the fast and slow components are $\tau_{o1} = 0.12$ ms (57.7%) and $\tau_{o2} = 0.94$ ms (42.3%) in the presence of $G\beta_1\gamma_7$ alone, and $\tau_{o1} = 0.49$ ms (55.3%) and $\tau_{o2} = 3.49$ ms (44.7%) in the presence of $G\beta_1\gamma_7$/Mg-ATP/PKA_c. The relative areas of individual components are given in parentheses. (*B*) Effect of PKA on scGIRK channel gating. A pair of an scGIRK and a K_{ACh} channel residing in the same membrane patch was activated in the presence of 4 nM $G\beta_1\gamma_7$, and then PKA_c was applied to the cytoplasmic side of the patch in the presence of Mg-ATP. Application of PKA triggered clustering of scGIRK channel openings into long bursts of activity. Expanded current traces recorded from the same patch before and after application of PKA are shown in the right panel to illustrate the kinetic behavior of the channel in greater detail. (*C*) All-points histograms generated from data recorded from the same scGIRK channel in the presence of $G\beta\gamma$ (*left panel*) and $G\beta\gamma$/Mg-ATP/PKA_c (*right panel*). The histograms were fitted by the sum of two Gaussian functions to determine the unitary conductance of scGIRK channel (14.4 pS and 14.2 pS, respectively).

conditions, the analysis of single-channel recordings was started at the same time point in each experiment, 10 min after $G\beta_1\gamma_7$ application.

$G\beta_1\gamma_7$ activated the scGIRK channels in a concentration-dependent manner. At 0.4 nM of $G\beta_1\gamma_7$, only a few singular openings could be recorded within a 40-min interval (Fig. 1). As $G\beta_1\gamma_7$ concentration was raised, the probability of the channel being open increased (Fig. 2). This increase in the channel open probability, however, was also associated with a shift from exclusively singular openings to more complex patterns of channel activity.

To assess the gating of the scGIRK channels at different $G\beta_1\gamma_7$ concentrations, we implemented the routine developed previously by us for the analysis of heterogeneous K_{ACh} channel behavior (Ivanova-Nikolova et al., 1998). The homogeneous sections of continuous recordings were divided into consecutive 400-ms segments and two parameters—frequency of openings, f, and open probability, p_o—were calculated for each data segment and plotted versus time.

The p_o and f plots presented in Fig. 5 *A* illustrate the fluctuations in the open probability and the frequency of openings for the initial 20 s of the scGIRK channel recording shown in Fig. 2. The p_o and f values calculated from the individual 400-ms data segments were further used to generate f and p_o histograms. These histograms were used to determine the number of conducting conformations accessible to the scGIRK channel and to quantify the equilibrium among different channel conformations (Colquhoun and Hawkes 1981, 1983; Colquhoun and Sakmann, 1985).

Fig. 5 *B* provides a comparison of two p_o distributions obtained at different $G\beta_1\gamma_7$ concentrations. In the presence of 0.4 nM $G\beta_1\gamma_7$, a single gamma distribution $\Gamma\ (p)$ for the sum of two variables with the same exponential distribution,

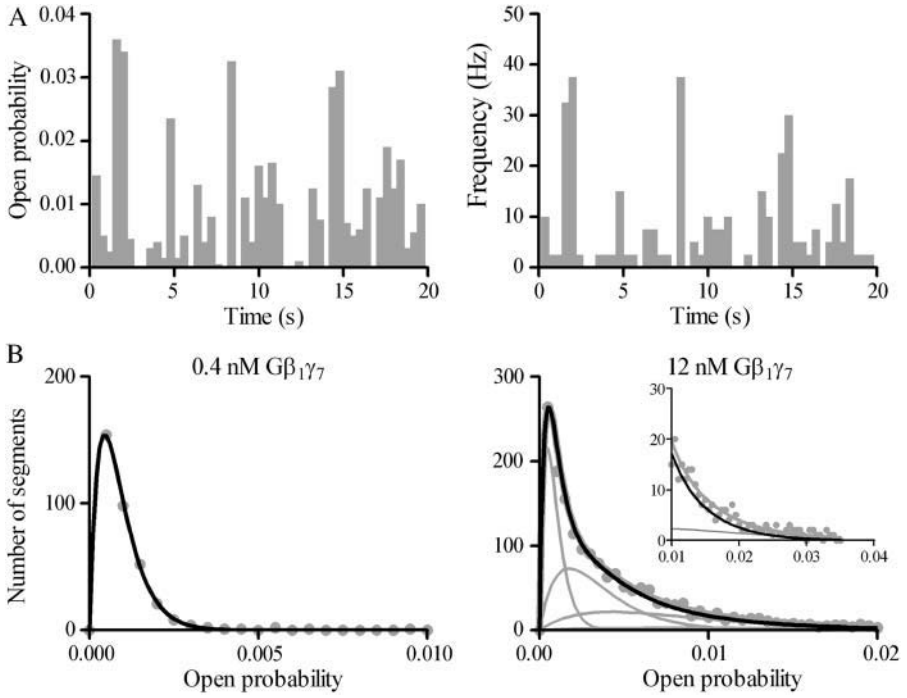

FIGURE 5 Classification of the scGIRK channel gating. (*A*) Continuous single-channel recordings were divided into consecutive 400-ms segments and the channel open probability and the frequency of openings were determined for the individual segments. Plots of open probability (*left panel*) and frequency of gating (*right panel*) versus time, derived from the initial 20 s of the scGIRK channel recording illustrated in Fig. 2, are shown to illustrate the heterogeneous channel behavior. (*B*) Modal classification of scGIRK channel gating. Open probability histograms generated from scGIRK channel activity recorded at two different $G\beta_1\gamma_7$ concentrations. The histogram shown at left was generated from pooled data recorded from four different scGIRK channels activated in the presence of 0.4 nM $G\beta_1\gamma_7$. The histogram shown at right was generated from data recordings from a single scGIRK channel activated in the presence of 12 nM $G\beta_1\gamma_7$. The histograms shown in this and the following figures leave out the blank 400-ms data segments and include the active data segments only. The p_o histograms were fitted by a sum of gamma components $\Gamma(p) = \Sigma N_k(p/p_{ok}^2)\exp(-p/p_{ok})$ to determine the mean p_o values and the relative occupancy of different gating components. The mean p_o values and relative areas (given in parentheses) of different components are $p_{o1} = 0.00045$ (100%) in the presence of 0.4 nM $G\beta_1\gamma_7$; and $p_{o1} = 0.00046$ (29.3%), $p_{o2} = 0.0018$ (37.7%), $p_{o3} = 0.0043$ (27.2%), and $p_{o4} = 0.0085$ (5.8%) in the presence of 12 nM $G\beta_1\gamma_7$. The inset shows the right part of the histogram on a different scale to illustrate the minor contribution of the component representing mode 4 (*gray line*) to the total fit of the histogram. This component was frequently too small to be accurately distinguished from the component representing mode 3, and therefore, modes 3 and 4 were analyzed together in the p_o histograms.

$p_o^{-1}\exp(-p/p_o)$, and mean p_o (Colquhoun and Sakmann, 1985) was sufficient to fit the p_o histogram, whereas the adequate fit of the p_o histogram generated in the presence of 12 nM $G\beta_1\gamma_7$ required a sum of four gamma components. Since each conducting conformation of an ion channel contributes a single kinetic component to the p_o and f histograms, our data suggest the presence of four conducting conformations or gating modes for each scGIRK channel. However, in the absence of PKA_c in the experimental chamber, even at saturating $G\beta_1\gamma_7$ concentrations the occupancy of gating mode 4 was very low (Fig. 5 *B*, *inset*). We therefore analyzed the gating in modes 3 and 4 together and the parameters estimated from the third gamma component in the p_o and f histograms were interpreted as a combined representation of the channel performance within these two modes.

The analysis of p_o and f histograms was also used to quantify the equilibrium probability (or relative occupancy) of individual gating modes. Different biochemical mechanisms may underline the complex gating behavior of an ion channel regulated by $G\beta\gamma$ binding. Previously, for the interpretation of heterogeneous K_{ACh} channel gating, we suggested that each gating mode, k, arises from binding of k $G\beta\gamma$ subunits to four equivalent and independent $G\beta\gamma$ sensors on a single tetrameric K_{ACh} channel (Ivanova-Nikolova et al., 1998). In this case, the probability of observing mode k should follow the binomial distribution,

$$P_k = [N!/k!(N-k)!]P^k(1-P)^{N-k}, \quad (1)$$

where P is the probability of $G\beta\gamma$ binding to one of the G-protein sensors, and $N = 4$. The equilibrium between the four functional modes of $G\beta_1\gamma_5$-activated K_{ACh} channels is in excellent agreement with the predictions of this model (Ivanova-Nikolova et al., 1998). Therefore, in this study we tested the possibility that different gating modes of the scGIRK channel arise from binding of one to four $G\beta\gamma$ subunits to four equivalent and independent $G\beta\gamma$ sensors in the scGIRK channel (Fig. 6 *A*). A simple test of this assumption would be to determine the correlation between the occupancies of individual gating modes. For each p_o and f histogram, the probability of $G\beta\gamma$ binding, P, was computed from the relative occupancy of mode 1, F_1, according to the equation

$$F_1 = 4P(1-P)^3/[1-(1-P)^4]. \quad (2)$$

Then the relative occupancy of the remaining k modes, F_k, was examined as a function of the parameter P. Fig. 6 *B* illustrates the results from this test for scGIRK and K_{ACh} channels activated in the same range of $G\beta_1\gamma_7$ concentrations.

The equilibrium analysis indicated that the theoretically derived binomial distributions for the probability of

observing gating modes 2, and 3 and 4 (Fig. 6 *B*, *solid lines*) superimposed upon the experimental F_k estimates (*symbols*) for both GIRK channels. We next investigated whether selecting a different gating mode as the basis for calculation of parameter P might influence its value. To test this possibility the probability of $G\beta_1\gamma_7$ binding to one of the $G\beta\gamma$ sensors, P, was computed from the relative occupancy of mode 2 in each experiment, F_2, according to the equation: $F_2 = 6P^2(1-P)^2/[1-(1-P)^4]$. Unlike the occupancy of mode 1, which provides a single P value for each F_1, the occupancy of mode 2 provides two P estimates for each F_2 value. To avoid this ambiguity in the interpretation of the occupancy of mode 2, for each histogram we selected the P value corresponding to the smaller difference, $(F^E_{3\&4} - F^T_{3\&4})$, where $F^E_{3\&4}$ and $F^T_{3\&4}$ are the experimentally determined and the theoretical occupancies of modes 3 and 4, respectively. This analysis revealed that the P value derived from each histogram was independent of the mode selected for its calculation, and thus confirmed the excellent compatibility between the model illustrated in Fig. 6 *A* and the gating equilibria of GIRK channels. In most recordings, however, the proportion of blank data segments significantly exceeded the probability of observing gating mode 0 (no $G\beta\gamma$ bound to the channel) calculated from the binomial distribution (Fig. 6 *B*). One possible reason for this deviation from the theoretical curve could be a $G\beta\gamma$-dependent desensitization of GIRK channels. Consistent with this possibility is our recent finding that the native K_{ACh} channels form large signaling complexes with several regulatory proteins in the atrial membrane (Nikolov and Ivanova-Nikolova, 2004). Two of the proteins found in these complexes, RACK1 (receptor for activated C kinase) and βARK (β-adrenergic receptor kinase) can function as $G\beta\gamma$ scavengers and, thus, might contribute to GIRK channel desensitization.

Alternatively, the discrepancy between the predicted and experimentally determined fractions of blank data segments in our experiments might be attributed to the presence of an additional nonconducting conformation of the GIRK channels. Thus, we considered a paradigm in which both the vacant and the singly occupied GIRK channels are silent (Fig. 7 *A*). To test this model, we once again examined the relative occupancy of the gating modes 1, 2, and 3 as a function of the probability of $G\beta\gamma$ binding, P. In this case, the parameter P, however, was computed from the relative occupancy of mode 0, F_0, according to the equation: $F_0 = 4P(1-P)^3 + (1-P)^4$. The results from this analysis (Fig. 7

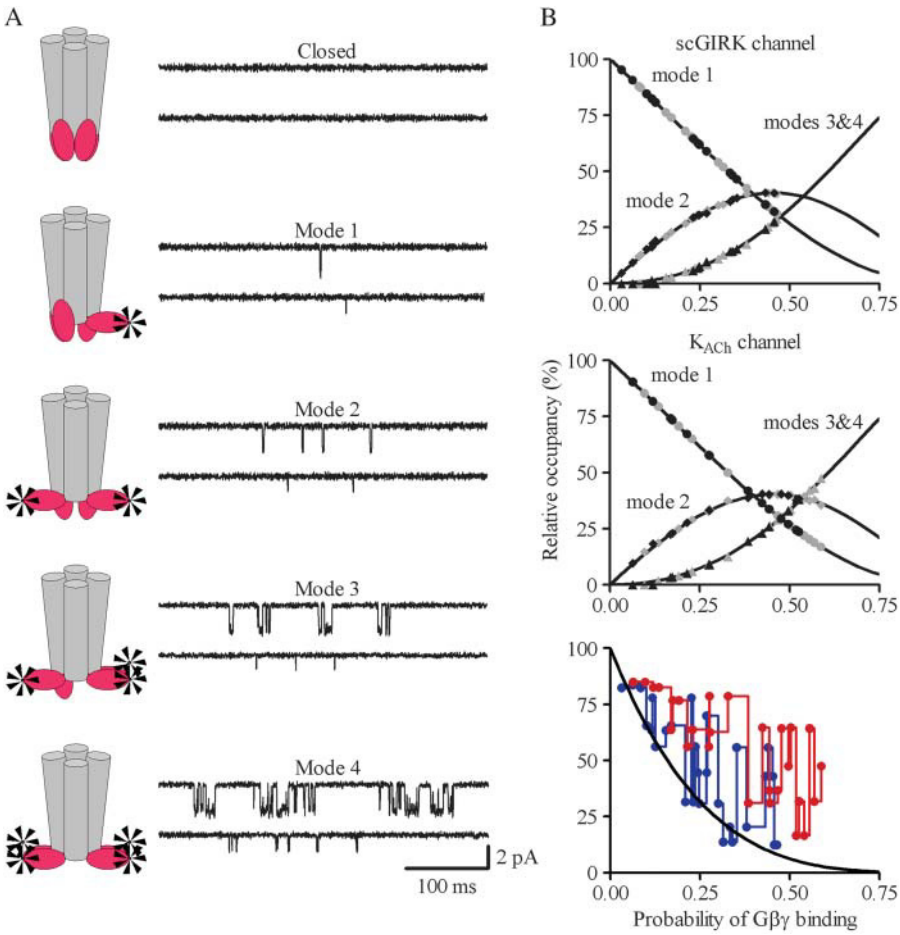

FIGURE 6 Gating equilibrium among four functional modes of GIRK channels. (*A*) A model assuming four functional modes of GIRK channels rendered active by the independent binding of an increasing number of $G\beta\gamma$ subunits to four equivalent $G\beta\gamma$ sensors in the channel structure. (*B*) For each channel, the relative occupancy of different gating modes was estimated from the fraction of the p_o (*gray symbols*) and f (*black symbols*) histograms fitted by the corresponding gamma components. The sojourns of the channels to gating modes 3 and 4 are jointly represented. In each experiment, the probability of $G\beta_1\gamma_7$-binding to one of the $G\beta\gamma$ sensors, P, was computed from the relative occupancy of mode 1, F_1, according to Eq. 2. The solid lines represent the predicted occupancy of the individual gating modes. The symbols represent the occupancy of mode 1 (*circles*), mode 2 (*diamonds*), and modes 3 and 4 (*triangles*) determined from the individual p_o and f distributions for different scGIRK ($n = 14$) and K_{ACh} ($n = 14$) channels. The graph in panel *B*, *bottom*, illustrates the discrepancy between the predicted occupancy of mode 0 and the experimentally determined fractions of blank data segments for the scGIRK (*blue*) and K_{ACh} (*red*) channels.

B) indicate that such a model reasonably well predicts the occupancy of all gating modes in the low $G\beta_1\gamma_7$ concentration range (0.4–1.6 nM) used in our experiments. At higher $G\beta_1\gamma_7$ concentrations, however, the relative occupancy of individual gating modes significantly deviated from the predicted binomial distribution.

Further, we sought to determine whether selecting a different gating mode for computation of the P values in the alternative model of GIRK channel gating shown in Fig. 7 *A* would improve the correlation between the theoretical distributions and the experimental F_k values. We therefore computed the P values from the occupancy of mode 1, F_1, according to the equation $F_1 = 6P^2(1 - P)^2$, and examined the relative occupancy of modes 0, 2, and 3 as a function of the parameter P. Our analysis indicated that the selection of a different mode for calculating the probability of Gβγ binding, P, did not improve the compatibility of our data with this model (data not shown). Nevertheless, the existence of nonconducting conformations of the singly occupied GIRK channels might be a viable option in the interpretation of channel behavior in the presence of different signaling partners of the GIRK channels and will be further tested.

Thus, the overall analysis of scGIRK channel activation by purified recombinant $G\beta_1\gamma_7$ supports the concept of channel gating in four conformations rendered active by the binding of an increasing number of Gβγ subunits to four seemingly identical and independent G-protein sensors on this channel. At the same time, we cannot rule out the possibility that the biochemical mechanisms underlying this heterogeneous GIRK channel behavior are much more complex, yet their consequences could be adequately explained by the simple idea entertained in this work.

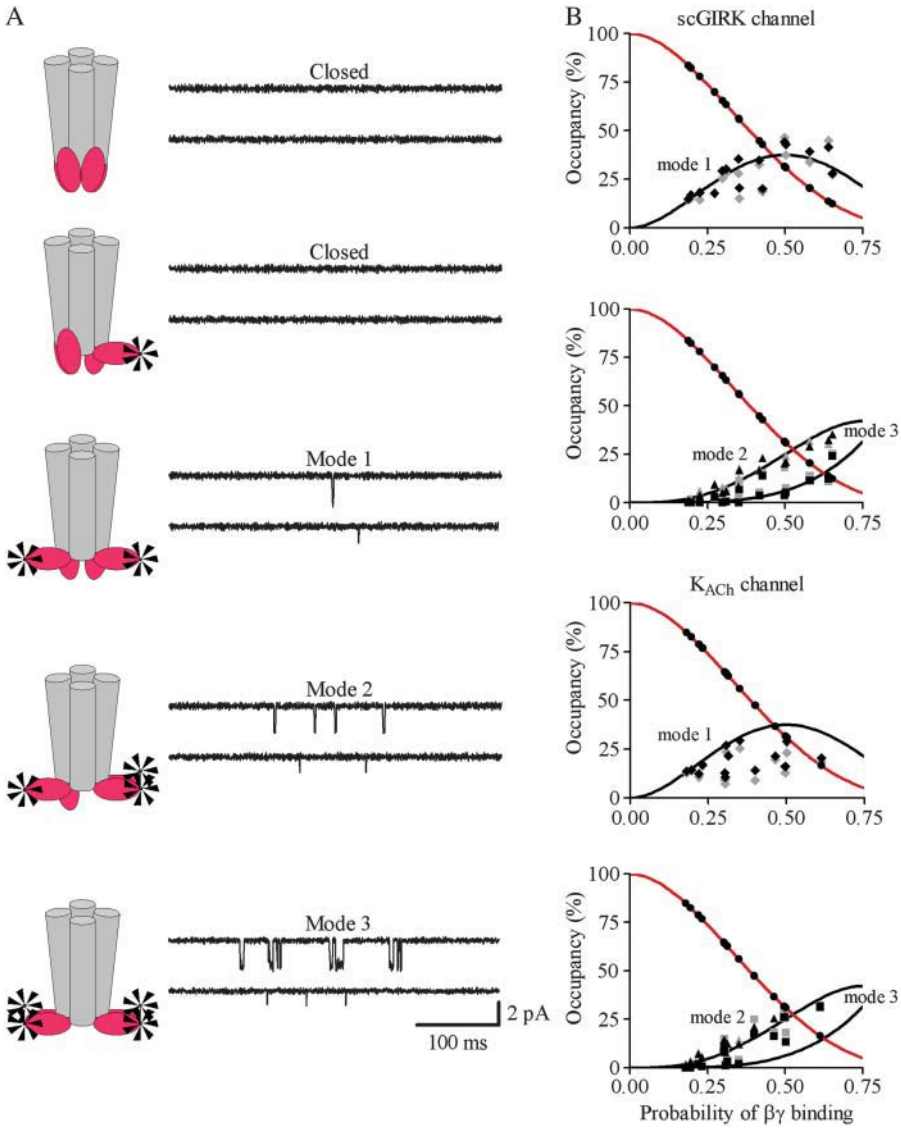

FIGURE 7 Gating equilibrium among three functional modes of GIRK channels. (*A*) A model assuming three functional modes of GIRK channels rendered active by the independent binding of two, three, and four Gβγ subunits to four equivalent Gβγ sensors in the channel structure. (*B*) For each channel, the relative occupancy of different gating modes was estimated from the fraction of the p_o (*gray symbols*) and f (*black symbols*) histograms fitted by the corresponding gamma components. In each experiment, the probability of $G\beta_1\gamma_7$-binding to one of the Gβγ sensors, P, was computed from the relative occupancy of mode 0, F_0, according to the equation: $F_0 = 4P(1 - P)^3 + (1 - P)^4$ (*red line*). The solid lines represent the predicted occupancy of the individual gating modes. The symbols represent the occupancy of mode 1 (*diamonds*), mode 2 (*triangles*), and mode 3 (*squares*) determined from the individual p_o and f distributions for different scGIRK ($n = 14$) and K_{ACh} ($n = 14$) channels.

Affinity of scGIRK and K_{ACh} channels for $G\beta_1\gamma_7$ binding

Membrane colocalization of two GIRK channels with different abilities to generate hyperpolarization responses would provide the atrial myocyte with a powerful means to control the membrane sensitivity to m_2-muscarinic receptor stimulation by adjusting the affinity of these channels to $G\beta\gamma$. To compare the $G\beta\gamma$ dissociation constants (K_d) of scGIRK and K_{ACh} channels in the atrial membrane, we analyzed the concentration dependence of the probability, P, of $G\beta\gamma$ binding to one of the putative $G\beta\gamma$ sensors. In each experiment we estimated parameter P at three standard time points—10, 20, and 30 min after the $G\beta_1\gamma_7$ perfusion. The mean value of the three P estimates was used to generate a dose-response curve for scGIRK and K_{ACh} channels, respectively (Fig. 8 *A*).

The probability of $G\beta\gamma$ binding, P, is a sigmoidal function of $G\beta\gamma$ concentration, and a fit with the Hill equation

$$P = P_{max}/\{1 + (K_d/[G\beta_1\gamma_7])^N\} \quad (3)$$

yields a Hill coefficient, N, of 4 for both channels. The dissociation constant, K_d, was 1.55 nM for the scGIRK and 1.65 nM for the K_{ACh} channels. The latter value is similar to the K_d value reported earlier for native K_{ACh} channels and the same $G\beta\gamma$ combination (Wickman et al., 1994). Although the scGIRK and K_{ACh} channels had virtually equal $G\beta\gamma$ affinity, the mean open probability of each gating mode was ~3.8-fold smaller for the scGIRKs as compared to the K_{ACh} channels (Fig. 8 *B*). In addition, the maximum probability of $G\beta\gamma$ binding, P_{max}, declined from 0.52 for the K_{ACh} channels to 0.36 for the scGIRKs, thus defining different gating boundaries for the two channels and further limiting the efficacy of the scGIRK channels. Altogether, the analysis of atrial scGIRK channel, in the presence of $G\beta\gamma$ alone, provided a picture of an ion channel with a significant $G\beta\gamma$-binding capacity but with very limited electrogenic efficacy.

Relationship between K_{ACh} and scGIRK channels in the membrane of atrial myocytes

The presence of K_{ACh} and scGIRK channels with identical $G\beta\gamma$ affinities in the same myocytes raises the possibility that these channels might compete for binding to the free $G\beta\gamma$ available in the membrane. To test this possibility we investigated the relationship between scGIRK and K_{ACh} channels found in the same membrane patch. Examination of 14 GIRK channel pairs demonstrated that the scGIRK and K_{ACh} channels behaved as individual entities and the gating equilibrium of each channel was not affected by the presence of the other channel in the same patch.

On the other hand, the inspection of long episodes of single-channel data revealed the presence of slow modal transitions (Yakubovich et al., 2000) in the gating of scGIRK and K_{ACh} channels, and these slow modal transitions were frequently linked for the two channels (Figs. 9; 10, *A* and *B*; and see Fig. 12). For 13 out of the 14 individual scGIRK

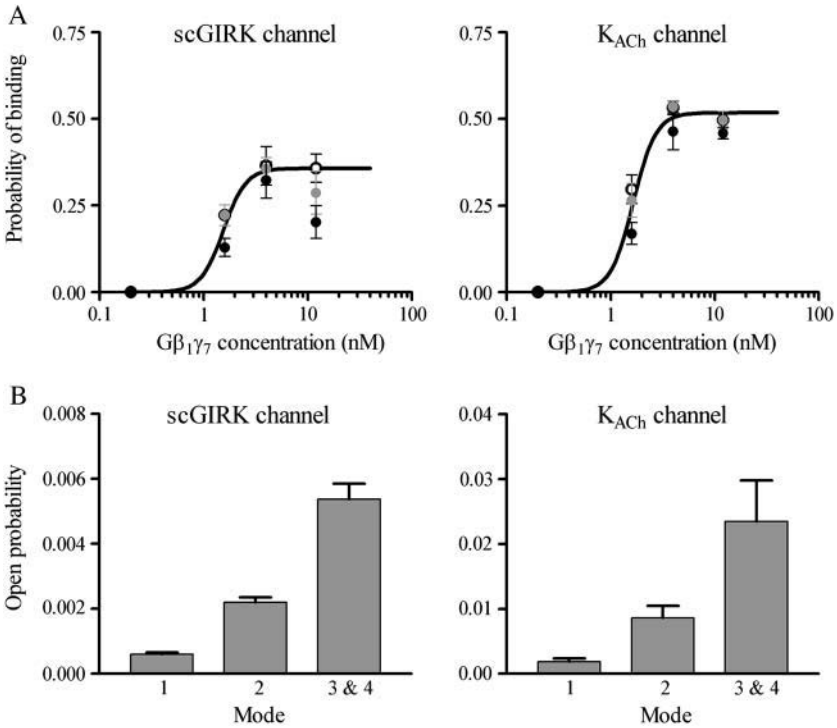

FIGURE 8 Comparison of the $G\beta_1\gamma_7$ affinity and electrogenic efficacy of the scGIRK and K_{ACh} channels. (*A*) $G\beta_1\gamma_7$ binding to scGIRK and K_{ACh} channels. The probability of $G\beta_1\gamma_7$ binding, P, is plotted against $G\beta_1\gamma_7$ concentration for the scGIRK (*left panel*) and K_{ACh} (*right panel*) channels. The parameter P was estimated at three standard time points of each experiment: 10 (*black circle*), 20 (*gray circle*) and 30 (*empty circle*) min after $G\beta_1\gamma_7$ perfusion. The points and error bars represent the mean ± SEM of four to six separate experiments. The solid lines through the data represent the least-squares fit with the Hill equation (Eq. 3), with a Hill coefficient, N, of 4 for both channels. The P_{max} constant is 0.52 for the K_{ACh} channel and 0.36 for the scGIRK channel, whereas the dissociation constant K_d is 1.65 nM for the K_{ACh} channel and 1.55 nM for the scGIRK channel. (*B*) Open probability of different gating modes. The mean open probabilities determined from the analysis of scGIRK p_o histograms (*left panel*) are $p_{o1} = 0.00060 \pm 0.00006$, $p_{o2} = 0.0022 \pm 0.0002$, and $p_{o3\&4} = 0.0054 \pm 0.0005$. The values for the K_{ACh} channel functional modes (*right panel*) are $p_{o1} = 0.0019 \pm 0.0005$, $p_{o2} = 0.0086 \pm 0.0018$, and $p_{o3\&4} = 0.0234 \pm 0.0063$. Data are mean ± SEM ($n$ = 10–14).

channels monitored at a constant $G\beta_1\gamma_7$ concentration for at least 20 min each, an initial period of infrequent but stable scGIRK gating was followed by a period of more appreciable channel activity (Fig. 10 *A*). Such transitions in scGIRK channel gating from low to high levels of activity were frequently coupled to slow modal transitions in K_{ACh} channel gating. Intriguingly, the K_{ACh} channels were able to undergo transitions in both directions: from low to high (Fig. 9) and from high to low level of activity (Fig. 12). In the set of 14 patches, seven displayed a synchronized increase in the activity of both channels (Fig. 10, *A* and *B*), whereas five patches displayed a reduction of K_{ACh} channel activity after the upregulation of scGIRK channels. In the remaining two patches the activity of the K_{ACh} channels was stable for the duration of the experiments.

The slow modal transitions in the gating of GIRK channels led to changes in the equilibrium between the four functional modes of these channels. Fig. 11 provides a direct comparison of the p_o histograms generated from the different phases of the experiment illustrated in Fig. 9, whereas the p_o histograms generated from the different phases of the experiment illustrated in Fig. 12 are shown in Fig. 13. The analysis of these p_o distributions revealed significant changes in the equilibrium probability of different functional modes, consistent with changes in the probability of Gβγ binding to the protein complexes. In addition, in some of our experiments, the slow modal transitions in GIRK channel gating affected the open probability of the individual gating modes (Figs. 11 and 13).

Two basic conclusions can be drawn from these observations. First, the Gβγ sensitivity of both channels appears to be a rather dynamic parameter controlled by yet unrecognized membrane components. As a result, the amplitude of hyperpolarization response of atrial myocytes to uniform receptor stimulation would greatly vary, depending not only on the relative density of the K_{ACh} and scGIRK channels in the membrane, but also on their relative Gβγ affinity at any particular moment. Second, there are at least two different membrane-delimited factors (or combinations of factors) that might modify the sensitivity of GIRK channels to Gβγ stimulation. In our experiments, one of these factors was apparently capable of amplifying the activity of both channels, whereas the other factor upregulated the scGIRK channels while inhibiting the K_{ACh} channel activity. Further studies are needed to identify these factors and to delineate their precise mechanism of action.

DISCUSSION

In this work we characterized the function of a previously unidentified Gβγ-sensitive inwardly rectifying channel in the heart, which we designated the scGIRK channel. These

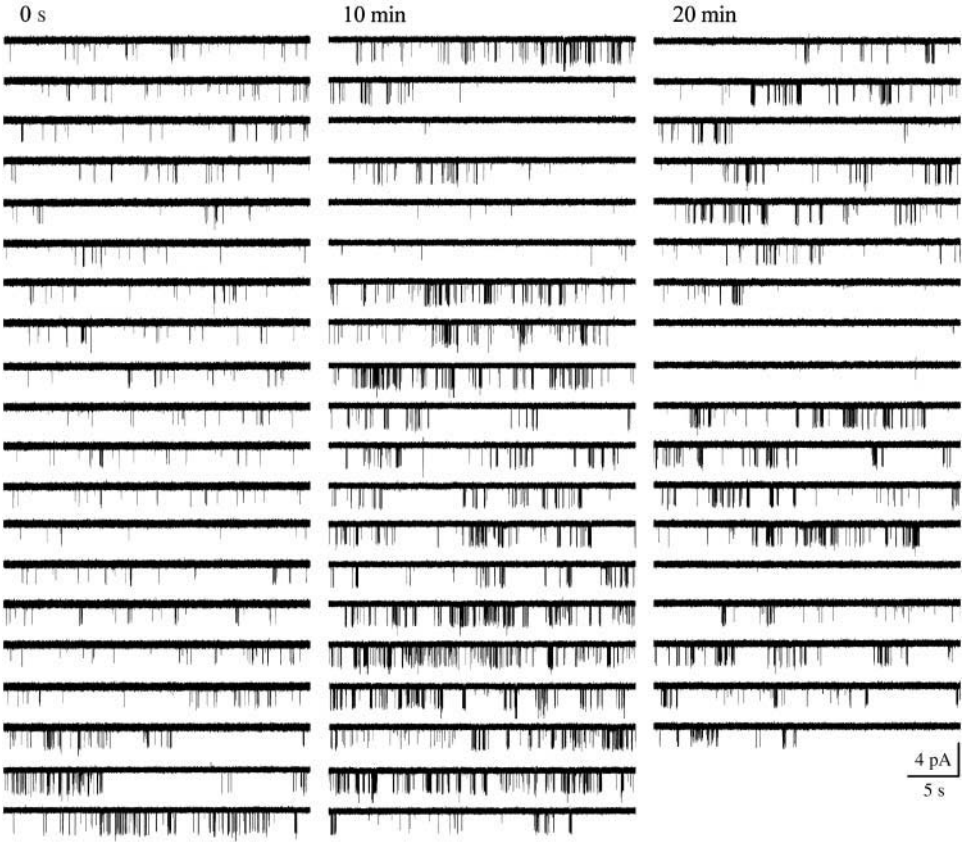

FIGURE 9 Synchronized slow modal transitions in GIRK channel gating. Single-channel recordings from a pair of scGIRK and K_{ACh} channel activated by 4 nM $G\beta_1\gamma_7$. After an initial period (~7 min) of steady gating, the activity of both channels increased simultaneously.

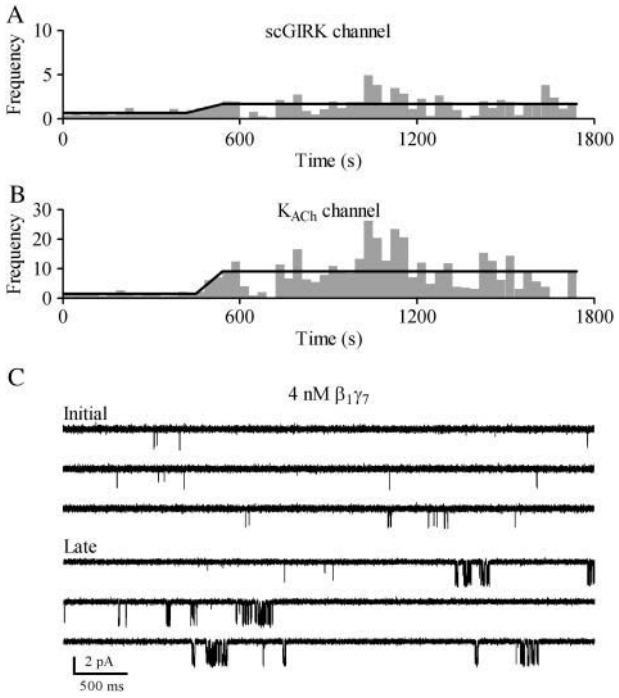

FIGURE 10 Biphasic activation of GIRK channels. Time courses of G$\beta\gamma$ activation for the scGIRK (*A*) and the K_{ACh} (*B*) channels shown in Fig. 9. To identify the different phases of scGIRK and K_{ACh} channel activation, the *F-t* plots were generated as described in Materials and Methods. The horizontal lines indicate the mean *F* values obtained within apparently homogeneous sections of channel activity. After an initial period (~7 min) of steady gating, the activity of both channels increased simultaneously. (*C*) Two representative 15-s segments of single-channel recordings are shown to illustrate the changes in the channel behavior associated with different phases of this experiment.

channels are expressed in the membrane of atrial myocytes and are frequently localized in close proximity to the classical K_{ACh} channels. The scGIRK channels are characterized by a unitary conductance of ~16 pS (with symmetrical 150-mM KCl solutions), very low open probability, and brief open states defined by two time constants, τ_{o1} and τ_{o2}, of 0.31 ms and 1.3 ms, respectively. Apparently, the small conductance combined with the low open probability would prevent the scGIRK channels from generating significant levels of hyperpolarization current in the atrial membrane.

Common gating mechanism for atrial GIRK channels

Upon G$\beta\gamma$ activation the scGIRK and K_{ACh} channels exhibit a complex behavior, fluctuating between different patterns of gating. This behavior is dependent on the G$\beta\gamma$ concentration. At G$\beta_1\gamma_7$ concentrations <1 nM, GIRK channel gating is characterized by infrequent, mostly singular openings. However, the channel activity begins to oscillate between singular openings and heterogeneous bursts of openings as the G$\beta\gamma$ concentration increases. Such heterogeneity of channel gating is a major obstacle in the interpretation of the single-channel recordings from both scGIRK and K_{ACh} channels. To quantify the complex gating of G$\beta\gamma$-activated K_{ACh} channels we previously developed a simplistic approach for classification of channel gating in functionally distinct modes (Ivanova-Nikolova et al., 1998). The recordings were divided into consecutive, equally spaced time intervals and the channel frequency of openings and the channel probability of being open were assessed within these intervals. The f and p_o values obtained from this analysis were then compiled to generate f and p_o histograms, and these histograms were used to evaluate the K_{ACh} channel-G$\beta\gamma$ interactions. In this study, the same approach was applied to classify the gating of scGIRK channels into individual functional modes. The results of our experiments indicated that although a single kinetic component was sufficient to approximate the f and p_o histograms at low G$\beta_1\gamma_7$ concentrations, a sum of up to four components was required for the adequate fit of the scGIRK channel data generated at saturating G$\beta_1\gamma_7$ concentrations. Thus, our analysis suggested the presence of four distinct gating modes not only for the K_{ACh} channels but for the scGIRKs as well.

In addition, the concentration dependence of the gating equilibrium is characteristic of an activation process driven by G$\beta\gamma$ concentration. Previously, for the K_{ACh} channels, we suggested that the multiple G$\beta\gamma$ binding sites identified in GIRK1 and GIRK4 subunits are arranged in a precise pattern to form four equivalent and independent G$\beta\gamma$ sensors in the channel structure (Ivanova-Nikolova et al., 1998). Additionally, we suggested that binding of one to four G$\beta\gamma$ subunits to these sensors gives rise to four distinct K_{ACh} channel conformations underlying the four gating modes. Several studies from different laboratories provided further support for the basic premises of this concept. The recent crystal structure of GIRK1 tetrameric cytoplasmic pore revealed the presence of four identical putative G$\beta\gamma$ sensors protruding from the pore (Nishida and MacKinnon, 2002). Similar structural organization is most probably conserved throughout the entire GIRK channel family. In addition, the existence of equilibrium between single-, double-, triple-, and quadruple-G$\beta\gamma$ occupied GIRK4 homotetramers was directly validated through biochemical experiments (Corey and Clapham, 2001). Furthermore, mutagenesis analysis of neuronal GIRK2 channels identified several mutations within GIRK2 transmembrane domains, which not only rendered the channels constitutively active but also confined their gating to individual gating modes (Yi et al., 2001). This last observation supports the notion that each gating mode represents a distinct configuration of the K_{ACh} channel protein.

In this study, we extended our concept of K_{ACh} channel gating to rationalize the modal behavior of the scGIRK channels. As long as the four gating modes can be viewed as manifestation of single-, double-, triple- and quadruple-G$\beta\gamma$

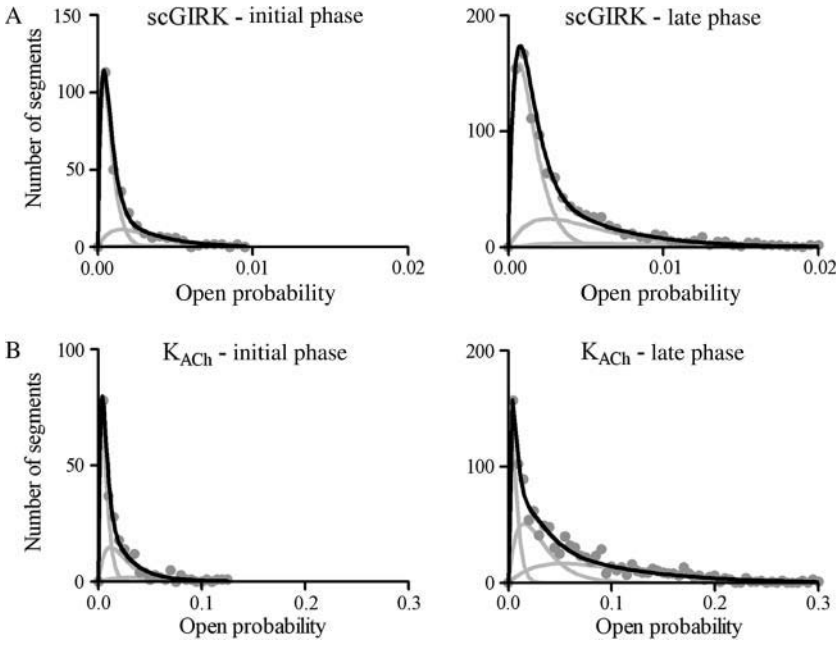

FIGURE 11 The slow modal transitions in scGIRK and K_{ACh} channel gating are associated with changes in the equilibrium among the four functional modes of these channels. (*A*) Open probability histograms generated from the initial (*left panel*) and late (*right panel*) phases of scGIRK activity shown in Fig. 9. The mean p_o values and the relative areas of different gamma components (shown in parentheses) are $p_{o1} = 0.00037$ (65.5%), $p_{o2} = 0.0015$ (28.7%), and $p_{o3} = 0.0032$ (5.8%) for the initial phase; and $p_{o1} = 0.00072$ (58.7%), $p_{o2} = 0.0026$ (32.8%), and $p_{o3} = 0.0045$ (8.5%) for the late phase of channel activation. The *P* values computed from these histograms are $P^{initial} = 0.225$, and $P^{late} = 0.270$. In this experiment, the changes in the kinetic behavior of the scGIRK were associated with both a slight shift in modal equilibrium and a significant increase in the open probability of different functional modes. (*B*) Open probability histograms generated from the initial (*left panel*) and late (*right panel*) phases of K_{ACh} channel activity shown in Fig. 9. The mean p_o values and the relative areas of different components are $p_{o1} = 0.0033$ (50.0%), $p_{o2} = 0.012$ (37.5%), and $p_{o3} = 0.031$ (12.5%) for the initial phase; and $p_{o1} = 0.0033$ (20.3%), $p_{o2} = 0.015$ (37.4%), and $p_{o3} = 0.053$ (42.3%) for the late phase of channel activation. The *P* values computed from these histograms are $P^{initial} = 0.328$ and $P^{late} = 0.555$ for the K_{ACh} channel. Thus, the changes in the gating behavior for this K_{ACh} channel were mostly associated with a shift in the modal equilibrium toward gating modes 3 and 4.

occupied scGIRK channels, the probability of observing each gating mode should be a function only of the probability of Gβγ binding to one of the four Gβγ sensors, *P*. To test this prediction we examined the gating equilibrium of scGIRK channels activated at different Gβγ concentrations. The parameter *P* was computed from the relative occupancy of mode 1, and the relative occupancy of remaining modes was examined as a function of *P* (Fig. 6). This examination demonstrated that the probability function of each of the remaining gating modes strictly followed the predicted binomial distribution (Eq. 1). Moreover, the selection of a different gating mode for the computation of parameter *P* did not influence the *P* values derived from the different *f* and p_o histograms, thus further confirming the excellent compatibility between the data and the model.

Analysis of the concentration dependence of gating equilibrium also demonstrated that the probability of one of the four Gβγ sensors being occupied, *P*, is a sigmoidal function of Gβγ concentration for both scGIRK and K_{ACh} channels. Remarkably, the two channels have identical $G\beta_1\gamma_7$ affinity (K_d of ~1.6 nM). This observation implies that not only the four Gβγ sensors of each scGIRK and K_{ACh} channel behave as equivalent and independent modules, but also that these sensors are structurally similar in scGIRK and K_{ACh} channels. However, the molecular identity of the Gβγ sensors (for reviews, see Yamada et al., 1998, and Sadja et al., 2003), and the conformational changes elicited in them upon Gβγ binding remain to be defined.

Although the scGIRK and K_{ACh} channels exhibited identical $G\beta_1\gamma_7$ affinities (Fig. 8 *A*), the electrogenic efficacy of the two channels was markedly different (Fig. 8 *B*). Thus, the same mechanism of Gβγ control of multiple functional states of single effector molecule is used to achieve a robust hyperpolarization response in the case of the K_{ACh} channels, and to generate a mute response in the case of the scGIRK channels.

Altogether, classification of scGIRK and K_{ACh} channel gating into four functional modes and subsequent analysis of equilibrium between the different modes greatly simplified the kinetic analysis of the heterogeneous single-channel data. This method was also sensitive enough to capture slight changes in Gβγ regulation of the two channels. However, as we previously reported (Ivanova-Nikolova et al., 1998), this method did not accurately predict the amount of blank data segments in the single-channel recordings throughout the entire Gβγ range. In the majority of our experiments, the fraction of blank data segments considerably exceeded the probability of observing gating mode 0 (no Gβγ bound to the channel), calculated from the binomial distribution (Eq. 1) for both channels. This observation indicates the presence of Gβγ-dependent desensitization in addition to the Gβγ-dependent activation of GIRK channels. The mechanism of the desensitization process, however, was not investigated in this work.

Although no attempt was made here to determine the molecular composition of the scGIRK channels, several lines

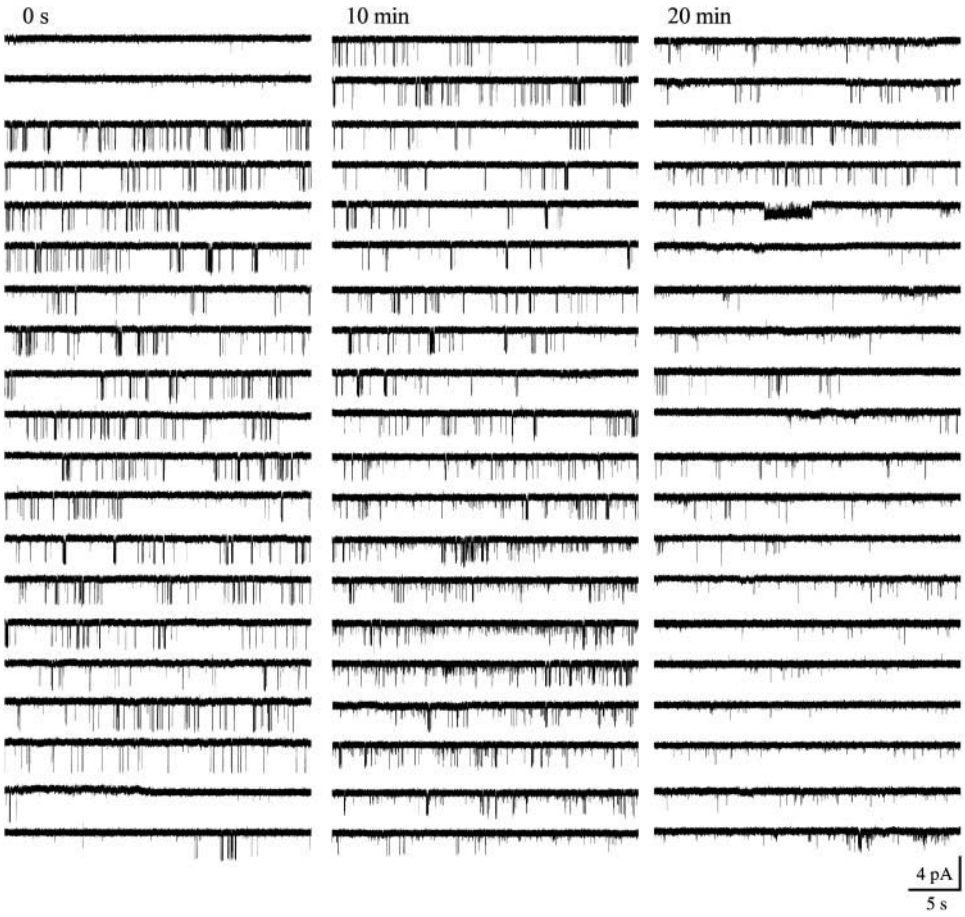

FIGURE 12 Opposing regulation of scGIRK and K_{ACh} channels. Single-channel activity recorded in the presence of 12 nM $G\beta_1\gamma_7$ from a membrane patch harboring a scGIRK and a K_{ACh} channel. In this experiment, an initial phase of efficient K_{ACh} channel gating and infrequent scGIRK openings was replaced with a second phase, characterized by increased scGIRK activity and infrequent K_{ACh} channel gating.

of evidence suggest that these channels might be functional GIRK4 homotetramers. The existence of GIRK4 homomultimers along with the GIRK1/GIRK4 heterotetramers has been demonstrated in the atria (Corey and Clapham, 1998). In addition, heterologous expression of GIRK4 homomultimers results in the formation of G-protein-regulated inwardly rectifying K^+ channels (Krapivinsky et al., 1995a,b). In these studies, however, the fast gating of the

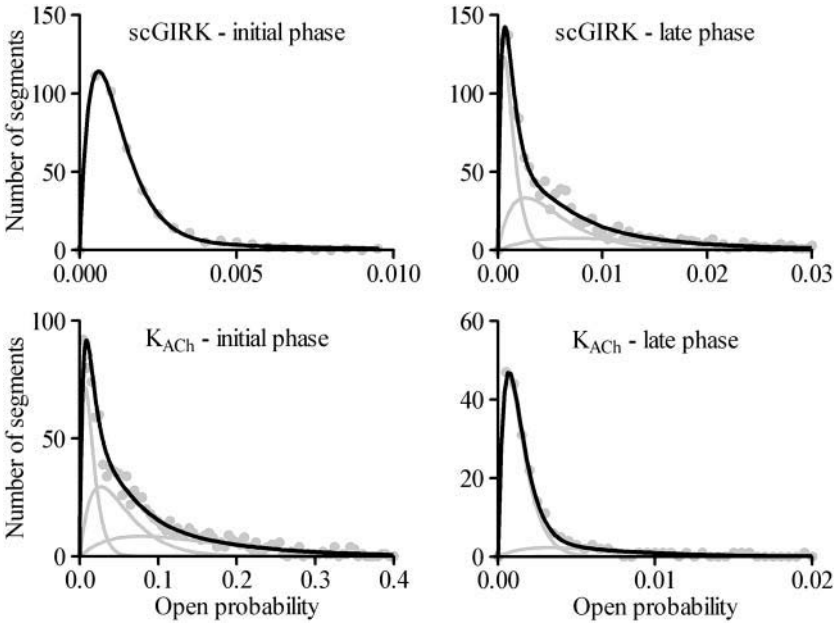

FIGURE 13 Modal distributions of scGIRK and K_{ACh} channels associated with the opposing regulation of these channels. Open probability histograms generated from the homogeneous phases of scGIRK (*top panels*) and K_{ACh} (*bottom panels*) channel gating shown in Fig. 12. For the scGIRK channel the mean p_o values and relative areas (given in parentheses) of different components are $p_{o1} = 0.00060$ (87.2%) and $p_{o2} = 0.0030$ (12.8%) for the initial phase; and $p_{o1} = 0.00061$ (34.3%), $p_{o2} = 0.0026$ (40.3%), and $p_{o3} = 0.0072$ (25.4%) for the late phase of channel activation. For the K_{ACh} channel the mean p_o values and the relative areas of different components are $p_{o1} = 0.0073$ (26.3%), $p_{o2} = 0.0268$ (40.0%), and $p_{o3} = 0.0780$ (33.7%) for the initial phase; and $p_{o1} = 0.00068$ (79.4%), $p_{o2} = 0.0032$ (18.7%), and $p_{o3} = 0.0080$ (1.9%) for the late phase of channel activation. The P values, determined from these distributions, are $P^{initial} = 0.084$ and $P^{late} = 0.440$ for the scGIRK channel; and $P^{initial} = 0.503$, and $P^{late} = 0.130$ for the K_{ACh} channel. The K_{ACh} channel gating during the late phase is impaired not only by its confinement within the low-efficient modes 1 and 2, but also by the significant reduction in the open probability of individual kinetic components contributing to channel activity.

recombinant GIRK4 channels impeded their analysis and prevented us from directly comparing the properties of GIRK4 homotetramers with those of atrial scGIRK channels. More recently, the properties of GIRK4 homomultimers were examined in *Xenopus* oocytes (He et al., 2002), and the analysis of GIRK4 channel openings resolved two components with time constants, τ_{o1} and τ_{o2}, of 0.26 ms and 0.89 ms, respectively. These estimates are very similar to the open-time constants for the scGIRK channels reported here. Finally, ion channels with biophysical properties identical to those of the scGIRK channels were observed in the atrial myocytes of GIRK1 knockout mouse after m_2-receptor activation (Bettahi et al., 2002). There are some differences, however, in the G-protein regulation of the atrial scGIRK channels and the residual GIRK4 homomultimers in the GIRK1 knockout mouse model. In the latter case, channel activity quickly ran down in cell-attached configuration after m_2-receptor activation and could not be reliably restored in inside-out patches by addition of GTP and ATP. These differences suggest that the presence of heterotetrameric K_{ACh} channels in the atrial membrane might be important for the function of GIRK4 homomultimers.

Despite these functional similarities between the scGIRK channels and the GIRK4 homomultimers, we cannot completely rule out the possibility that the 16-pS openings might result from transitions to a subconductance state of the GIRK1/GIRK4 heterotetrameric channel that is accessed from the closed state only. An alternative explanation might be that the scGIRK channels represent a yet unidentified covalent modification of the K_{ACh} channels. In any case, the presence of the scGIRK channels in the atrial membrane could have a major effect on the cellular responses to m_2-receptor stimulation.

Physiological role of scGIRK channels in the atrial membrane

The limited ability of the scGIRK channels to generate membrane current does not suggest a substantial role for these channels in the hyperpolarization of atrial myocytes. The examination of interactions between the scGIRK and canonical K_{ACh} channels, however, indicates that scGIRKs might create a gradient of hyperpolarization responses across atrial membrane. In fact, recent examination of acetylcholine-sensitive K^+ currents in myocytes from adult mouse atrium revealed a significant gradient of I_{KACh} current density across the supraventricular structures of the mouse heart (Lomax et al., 2003). The molecular mechanisms underlying this phenomenon are currently unknown but most likely involve different K_{ACh} channel densities in different supraventricular structures. At the same time, the interactions between scGIRK and K_{ACh} channels in the atrial membrane could be responsible for dynamic changes in the gradient of I_{KACh} current density across the atria, and thus might have significant clinical repercussions. These interactions would be determined by the proximity of the two channels and their ability to compete for binding to the pool of Gβγ subunits released upon receptor activation. The analysis of scGIRK and K_{ACh} channel activation revealed similar $G\beta_1\gamma_7$ affinities for the two channels which supports the notion that the two channels might indeed compete for Gβγ binding. Furthermore, it is well established that K_{ACh} channel activity is modulated by a large variety of intracellular factors and processes. These include phosphatidylinositol-4,5-bisphosphate, Na^+, Mg^{2+}, oxidation-reduction, phosphorylation-dephosphorylation, and protonation (reviewed in Dascal, 1997, and Sadja et al., 2003). Our limited experiments with PKA_c suggest that some of the same intracellular factors and processes might be involved in the regulation of the scGIRK channels too. Future studies will test this possibility.

This work was made possible by the generosity of Dr. Janet D. Robishaw (Weis Center for Research, Geisinger Medical Center, Danville, PA), in whose lab the purification of Gβγ was carried out. We thank Dr. D. Logothetis and his colleagues for kindly providing the numerical τ_{o1} and τ_{o2} values for the GIRK4 homomeric channels. We are extremely grateful to the two reviewers for their insightful comments, which led to a significant improvement of this manuscript.

This work was supported by a faculty development grant from Brody School of Medicine, East Carolina University.

REFERENCES

Bettahi, I., C. L. Marker, M. I. Roman, and K. Wickman. 2002. Contribution of the Kir3.1 subunit to the muscarinic-gated atrial potassium channel I_{KACh}. *J. Biol. Chem.* 277:48282–48288.

Colquhoun, D., and A. G. Hawkes. 1981. On the stochastic properties of single ion channels. *Proc. R. Soc. B.* 211:205–235.

Colquhoun, D., and A. G. Hawkes. 1983. The principles of the stochastic interpretation of ion-channel mechanisms. *In* Single Channel Recording. B. Sakmann, and E. Neher, editors. Plenum Press, New York. 135–175.

Colquhoun, D., and B. Sakmann. 1985. Fast events in single-channel currents activated by acetylcholine and its analogues at the frog muscle end-plate. *J. Physiol.* 369:501–557.

Corey, S., and D. E. Clapham. 1998. Identification of native atrial G-protein-regulated inwardly rectifying K^+ (GIRK4) channel homomultimers. *J. Biol. Chem.* 273:27499–27504.

Corey, S., and D. E. Clapham. 2001. The stoichiometry of Gβγ binding to G-protein-regulated inwardly rectifying K^+ channels (GIRKs). *J. Biol. Chem.* 276:11409–11413.

Dascal, N. 1997. Signalling via the G protein-activated K^+ channels. *Cell. Signal.* 9:551–573.

Dascal, N., W. Schreibmayer, N. F. Lim, W. Wang, C. Chavkin, L. Di-Magno, C. Labarca, B. L. Kieffer, C. Gaveriaux-Ruff, D. Trollinger, H. A. Lester, and N. Davidson. 1993. Atrial G protein-activated K^+ channel: expression cloning and molecular properties. *Proc. Natl. Acad. Sci. USA.* 90:10235–10239.

Doupnik, C. A., N. Davidson, H. A. Lester, and P. Kofuji. 1997. RGS proteins reconstitute the rapid gating kinetics of Gβγ-activated inwardly rectifying K^+ channels. *Proc. Natl. Acad. Sci. USA.* 94:10461–10466.

Doyle, D. A., J. H. Morais Cabral, R. A. Pfuetzner, A. Kuo, J. M. Gulbis, S. L. Cohen, B. T. Chait, and R. MacKinnon. 1998. The structure of the potassium channel: molecular basis of K^+ conduction and selectivity. *Science.* 280:69–77.

Foster, K. A., P. J. McDermott, and J. D. Robishaw. 1990. Expression of G proteins in rat cardiac myocytes: Effect of KCl depolarization. *Am. J. Physiol.* 28:H432–H441.

Hamill, O. P., A. Marty, E. Neher, B. Sakmann, and F. J. Sigworth. 1981. Improved patch-clamp techniques for high-resolution current recording from cells and cell-free membrane patches. *Pflugers Arch.* 391:85–100.

He, C., X. Yan, H. Zhang, T. Mirshahi, T. Jin, A. Huang, and D. E. Logothetis. 2002. Identification of critical residues controlling G protein-gated inwardly rectifying K^+ channel activity through interactions with the $\beta\gamma$ subunits of G proteins. *J. Biol. Chem.* 277:6088–6096.

Ito, H., T. Sugimoto, I. Kobayashi, K. Takahashi, T. Katada, M. Ui, and Y. Kurachi. 1991. On the mechanism of basal and agonist-induced activation of the G protein-gated muscarinic K^+ channel in atrial myocytes of guinea pig heart. *J. Gen. Physiol.* 98:517–533.

Ivanova-Nikolova, T. T., E. N. Nikolov, C. Hansen, and J. D. Robishaw. 1998. Muscarinic K^+ channel in the heart: Modal regulation by G protein $\beta\gamma$ subunits. *J. Gen. Physiol.* 112:199–210.

Jiang, Y., A. Lee, J. Chen, M. Cadene, B. T. Chait, and R. MacKinnon. 2002. The open pore conformation of potassium channels. *Nature.* 417:523–526.

Jin, T., L. Peng, T. Mirshahi, T. Rohacs, K. W. Chan, R. Sanchez, and D. E. Logothetis. 2002. The $\beta\gamma$ subunits of G proteins gate a K^+ channel by pivoted bending of a transmembrane segment. 2002. *Mol. Cell.* 10:469–481.

Kozasa, T., and A. G. Gilman. 1995. Purification of recombinant G proteins from Sf9 cells by hexahistidine tagging of associated subunits. *J. Biol. Chem.* 270:1734–1741.

Kim, D. 1990. β-Adrenergic regulation of the muscarinic-gated K^+ channel via cyclic AMP-dependent protein kinase in atrial cells. *Circ. Res.* 67:1292–1298.

Krapivinsky, G., E. A. Gordon, K. Wickman, B. Velimirovic, L. Krapivinsky, and D. E. Clapham. 1995a. The G-protein-gated atrial K^+ channel I_{KACh} is a heteromultimer of two inwardly rectifying K^+ channel proteins. *Nature.* 374:135–141.

Krapivinsky, G., L. Krapivinsky, B. Velimirovic, K. Wickman, B. Navarro, and D. E. Clapham. 1995b. The cardiac inward rectifier K^+ channel subunit, CIR, does not comprise the ATP-sensitive K^+ channel, I_{KATP}. *J. Biol. Chem.* 270:28777–28779.

Kubo, Y., E. Reuveny, P. A. Slesinger, Y. N. Jan, and L. Y. Jan. 1993. Primary structure and functional expression of a rat G-protein-coupled muscarinic potassium channel. *Nature.* 364:802–806.

Leaney, J. L., G. Milligan, and A. Tinker. 2000. The G protein α subunit has a key role in determining the specificity of coupling to, but not the activation of, G protein-gated inwardly rectifying K^+ channels. *J. Biol. Chem.* 275:921–929.

Lomax, A. E., R. A. Rose, and W. R. Giles. 2003. Electrophysiological evidence for a gradient of G protein-gated K^+ current in adult mouse atria. *Br. J. Pharmacol.* 140:576–584.

Mullner, C., D. Yakubovich, C. W. Dessauer, D. Platzer, and W. Schreibmayer. 2003. Single channel analysis of the regulation of GIRK1/GIRK4 channels by protein phosphorylation. *Biophys. J.* 84: 1399–1409.

Nikolov, E. N., and T. I. Ivanova-Nikolova. 2004. Coordination of membrane excitability through a GIRK1 signaling complex in the atria. *J. Biol. Chem.* 279:23630–23636.

Nishida, M., and R. MacKinnon. 2002. Structural basis of inward rectification: Cytoplasmic pore of the G protein-gated inward rectifier GIRK1 at 1.8 Å resolution. *Cell.* 111:957–965.

Peleg, S., D. Varon, T. Ivanina, C. W. Dessauer, and N. Dascal. 2002. $G\alpha_I$ controls the gating of the G protein-activated K^+ channel, GIRK. *Neuron.* 33:87–99.

Sadja, R., N. Alagem, and E. Reuveny. 2003. Gating of GIRK channels: Details of an intricate, membrane-delimited signaling complex. *Neuron.* 39:9–12.

Saitoh, O., Y. Kubo, Y. Miyatani, T. Asano, and H. Nakata. 1997. RGS8 accelerates G-protein-mediated modulation of K^+ currents. *Nature.* 390:525–529.

Silverman, S. K., H. A. Lester, and D. A. Dougherty. 1996. Subunit stoichiometry of a heteromultimeric G protein-coupled inward-rectifier K^+ channel. *J. Biol. Chem.* 266:19528–19535.

Sui, J. L., K. W. Chan, and D. E. Logothetis. 1996. Na^+ activation of the muscarinic K^+ channel by a G-protein-independent mechanism. *J. Gen. Physiol.* 108:381–391.

Tucker, S. J., M. Pessia, and J. P. Adelman. 1996. Muscarine-gated K^+ channel: subunit stoichiometry and structural domains essential for G protein stimulation. *Am. J. Physiol.* 271:H379–H385.

Wickman, K. D., J. A. Inigues-Lluhi, P. A. Davenport, R. Taussing, G. B. Krapivinsky, M. E. Linder, A. G. Gilman, and D. E. Clapham. 1994. Recombinant G-protein $\beta\gamma$ subunits activate the muscarinic-gated atrial potassium channel. *Nature.* 368:255–257.

Wickman, K., J. Nemec, S. J. Gendler, and D. E. Clapham. 1998. Abnormal heart rate regulation in *GIRK4* knockout mice. *Neuron.* 20:103–114.

Yakubovich, D., V. Pastushenko, A. Bitler, C. W. Dessauer, and N. Dascal. 2000. Slow modal gating of single G-protein-activated K^+ channels expressed in *Xenopus* oocytes. *J. Physiol.* 524:737–755.

Yamada, M. 2002. The role of muscarinic K^+ channels in the negative chronotropic effect of a muscarinic agonist. *J. Pharmacol. Exp. Ther.* 300:681–687.

Yamada, M., A. Inanobe, and Y. Kurachi. 1998. G protein regulation of potassium ion channels. *Pharmacol. Rev.* 50:723–757.

Yi, B. A., Y. F. Lin, Y. N. Jan, and L. Y. Jan. 2001. Yeast screen for constitutively active mutant G protein-activated potassium channels. *Neuron.* 29:657–667.